Snow and Water Imaging Spectrometer (SWIS): First alignment and characterization results

Holly A. Bender*, Pantazis Mouroulis, Justin Haag, Christopher D. Smith[a], Byron E. Van Gorp

Jet Propulsion Laboratory, California Institute of Technology, Pasadena, California, USA
[a]Sierra Lobo Inc., Pasadena, California, USA

ABSTRACT

The Snow and Water Imaging Spectrometer (SWIS) is a fast, high-uniformity, low-polarization sensitivity imaging spectrometer and telescope system designed for integration on a 6U CubeSat platform. Operating in the 350-1700 nm spectral region with 5.7 nm sampling, SWIS is capable of simultaneously addressing the demanding needs of coastal ocean science and snow and ice monitoring. New key technologies that facilitate the development of this instrument include a linear variable anti-reflection (LVAR) detector coating for stray light management, and a single drive on-board calibration mechanism utilizing a transmissive diffuser for solar calibration. We provide an overview of the SWIS instrument design and potential science applications and describe the instrument assembly and alignment, supported by laboratory measurements.

Keywords: imaging spectroscopy, Dyson spectrometer, CubeSat

1. INTRODUCTION AND SCIENCE APPLICATIONS

The Snow and Water Imaging Spectrometer (SWIS) is a science-grade imaging spectrometer suitable for CubeSat applications, spanning a 350-1700 nm spectral range with 5.7 nm sampling, a 10 degree field of view and 0.3 mrad spatial resolution. The system operates at F/1.8, providing the high throughput for low-reflectivity (<1%) water surfaces, while a high readout rate avoids saturation over bright snow (reflectivity >90%). A conceptualized image of the SWIS 6U CubeSat spacecraft is shown in Figure 1.

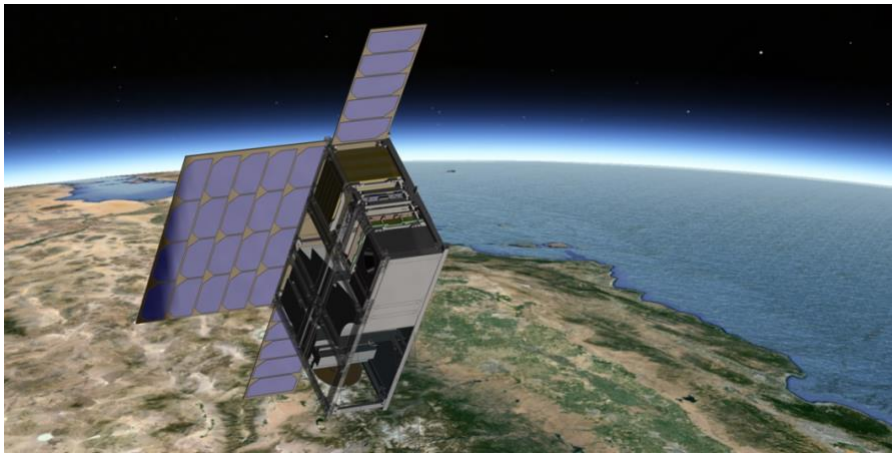

Fig 1: An artist's concept of the SWIS 6U CubeSat spacecraft, the spectrometer and telescope contained within the lower 4U

Corresponding author: *holly.a.bender@jpl.nasa.gov; Address: Jet Propulsion Laboratory, 4800 Oak Grove Drive, MS 306-392, Pasadena, CA, USA 91109.

The design utilizes heritage from previously demonstrated instruments on airborne (AVIRIS[1], MaRS[2], NGIS[3], PRISM[4]) and lunar (M3)[5] platforms, while advancing the state of the art in compact sensors of this kind in terms of size and spectral coverage. The CubeSat platform allows for more frequent and regular sampling compared to airborne campaigns, with intermediate to high resolution relative to heritage global sensors (typically having greater than 500 m resolution). SWIS is thus particularly well-suited for two critical science applications with temporal and spatially-varying properties that are distributed around the globe: coastal ocean and snow and ice. [6-9]

Significant science can be performed even with a single CubeSat carrying SWIS. For targets in polar regions (ie: Greenland's Jakobshavn Glacier and Antarctica Palmer Station, where SWIS could simultaneously map the controlling processes of glacier melt and the response of ocean biology to melt flux and nutrient loading), one SWIS spacecraft with ±20° pointing could achieve coverage in an alternating pattern of roughly 12 days on and 12 days off for half the year. In equatorial regions, access is closer to 1 week per month. However, extending the pointing to ±40° or adding a second satellite would increase coverage by a factor of 2. Daily coverage year-round would be achieved with 4-6 spacecraft. For a more thorough examination of potential mission concepts, see Ref. 10.

Two key science questions we can address with a single CubeSat carrying SWIS include:

1. What is the spatial extent and frequency of various types of episodic blooms throughout regions of the globe, and how are their formation and duration linked to environmental forcing mechanisms?

2. What are the controls on absorbed solar radiation in snow and ice by grain size variation and radiative forcing by dust and black carbon to within daily mean of 3 W m-2?

SWIS is capable of achieving this, and other assessments on ecosystem changes, cryosphere melt behavior and the impacts of climate change and human activities on coastal regions, through frequent repeat observations from space at a moderate spatial resolution.

2. SPECIFICATIONS

The SWIS instrument consists of a three-mirror anastigmat (TMA) telescope and Dyson form spectrometer and is designed for compatibility with a 6U CubeSat frame (Fig. 2). The 100mm focal length telescope provides 160 m resolution from an orbit of 500 km and is the highest resolution form able to fit in the 6U frame without deployable mirrors. Utilizing the Dyson form spectrometer allows us to achieve the compact size required for CubeSat-compatibility while providing a low F-number and high throughput. A spectral range of 350-1700 nm with 5.7 nm sampling satisfies coastal ocean targets with spectral features of interest mainly falling below 0.9 μm[6], as well as snow and ice targets, which contain critical features from the visible into the near- and shortwave-infrared.[8,9] A single-drive on-board calibration mechanism provides accurate calibration using solar and lunar views.[11]

System specifications are shown in Table 1, with predicted signal to noise in Fig. 3. Details of the optical design are discussed in greater detail in Ref. 12, while the calibration mechanism and optomechanical design considerations are addressed in Ref. 13.

SWIS generates data at a rate of roughly 25 Mbps (at 14 bits), assuming the latest JPL band-specific 4x lossless compression techniques. One square patch 90 x 90 km is approximately 6 Gb of data, and a 90 x 900 km strip is 60 Gb. This can be downloaded with a CubeSat X-band transmitter at 100Mbps with a total download of approximately 13GB per orbit as per Ref. 14, accessed in July 2017.

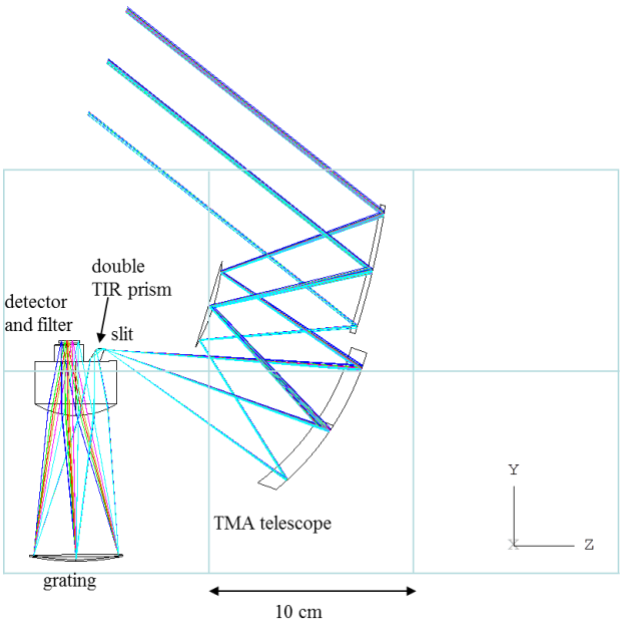

Figure 2: Spectrometer and telescope raytrace overlaid with a 20 cm x 30 cm rectangular footprint, approximating a 6U CubeSat frame. The frame extends 10 cm in the x-direction, and telescope mirror size is maximized within that available space. The folding arrangement is made possible by a small prism used in dual total internal reflection.

Table 1: SWIS system specifications

Property	**Value**
Spectral range	350-1700 nm
Spectral sampling	5.7 nm (/30 μm)
Cross track spatial elements	600 (+40 monitor)
Uniformity	95%
Resolution	0.3 mrad or 150 m from 500 km orbit
Working F-number	1.8
Cross track FOV	10° (±20° pointing) or 90 km from 500 km orbit
SNR	See plot in Fig. 3

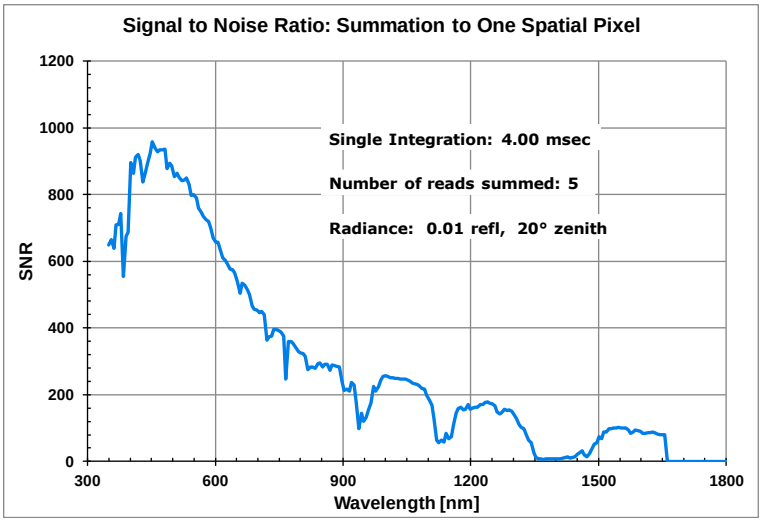

Fig. 3: SWIS Signal to Noise Ratio given 4ms integration time, summed 5x to one pixel, target R = 0.01, 20$_{o}$ zenith angle.

3. ASSEMBLY AND ALIGNMENT

The SWIS instrument has been fully assembled with the interferometrically aligned telescope (Fig. 4) and optomechanically assembled Dyson spectrometer and calibration mechanism (Fig. 5) mated and installed onto a rotation stage for integration into a thermal vacuum chamber (Fig. 6).

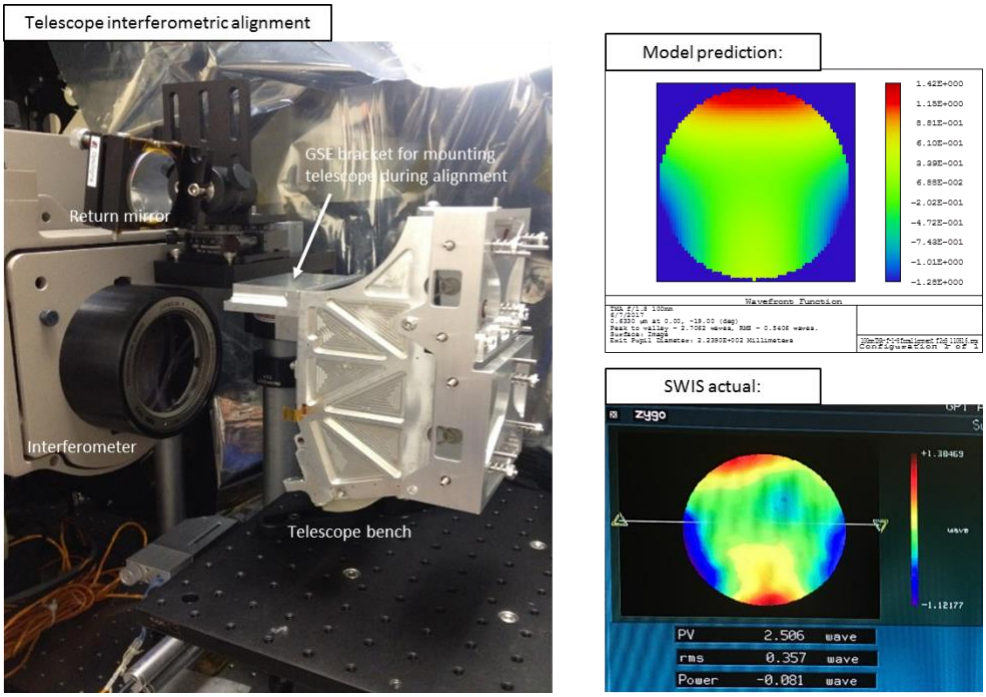

Fig. 4: The SWIS TMA telescope was aligned interferometrically *(left)* using tooling balls to set the interferometer focus to the instrument slit location. With the telescope secondary mirror stationary, the primary and tertiary mirrors were adjusted until a good interferometric match with the model prediction was achieved *(right).*

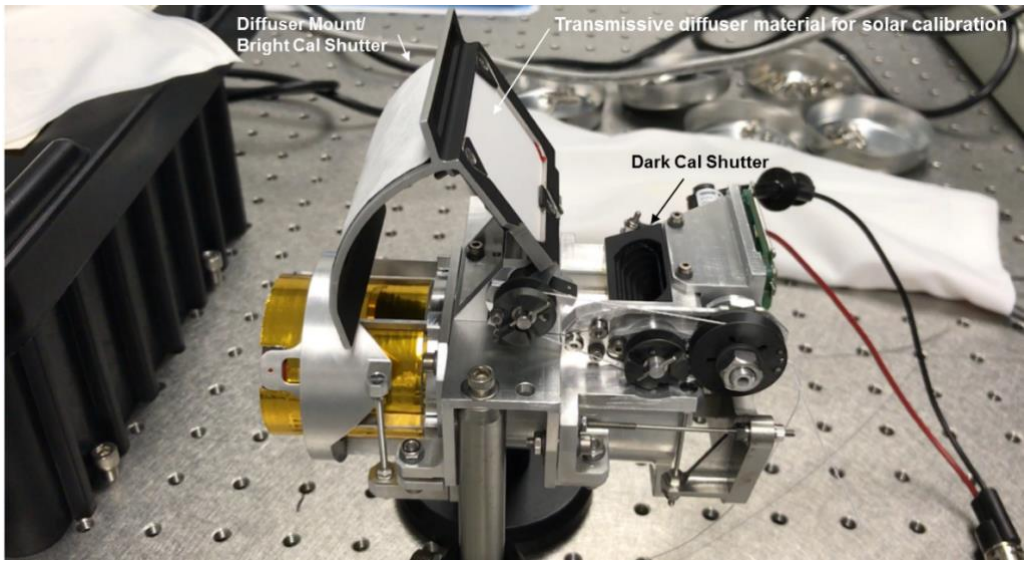

Fig. 5: Assembled Dyson spectrometer with the calibration mechanism in the science position. For solar calibration, the Bright Cal Shutter blocks light from the telescope while a transmissive diffuser material passes sunlight into the spectrometer. The material, Heraeus OM100 is Lambertian enough to achieve stable illumination without a need for highly accurate CubeSat pointing. The Dark Cal Shutter is closed for dark frames.

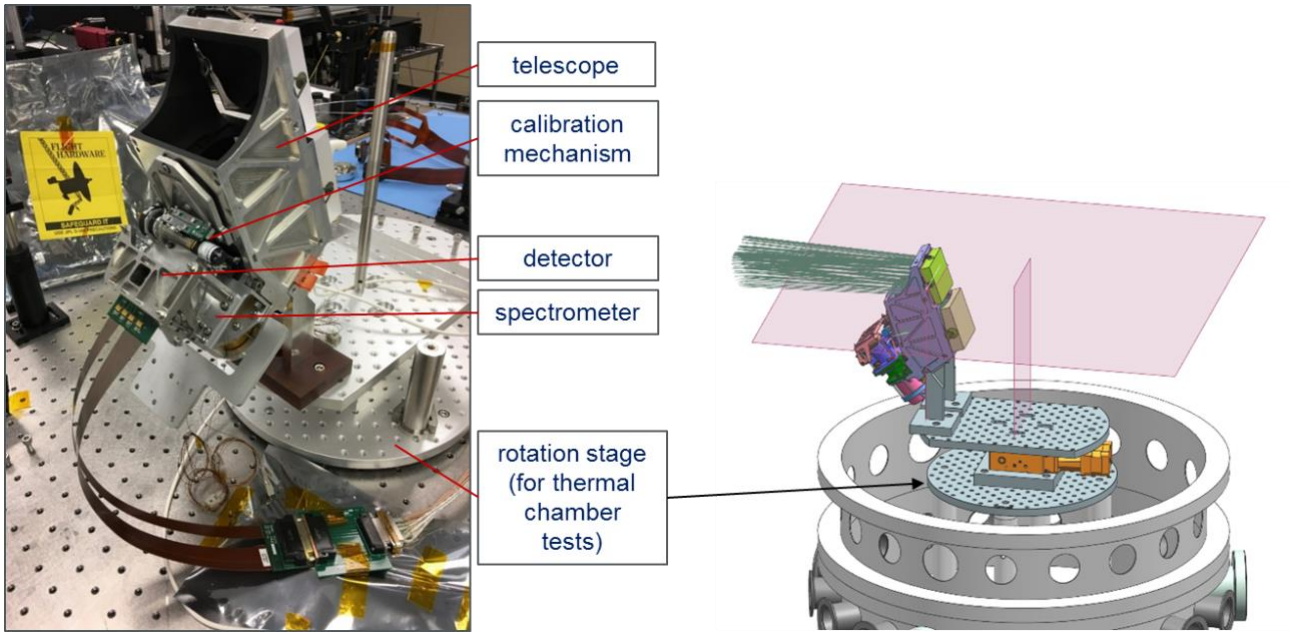

Fig. 6: The full optical assembly with the spectrometer mated to the telescope sits on a rotation stage ready for integration into a thermal vacuum chamber for final alignment and thermal testing.

Preliminary alignment of the detector's six degrees of freedom, grating clocking, and telescope-to-spectrometer focus was achieved at room temperature prior to integration into the chamber. Our HgCdTe detector was optimized by Teledyne Scientific & Imaging for high temperature (~250 K) operation in order to allow SWIS to operate without cryocoolers. As an added benefit, this allowed us to utilize the detector at room temperature to perform substantial preliminary alignment before integration into our thermal vacuum chamber, saving time and resources. The alignment presented here was achieved after two thermal cycles. The measurement of key spectral and spatial response functions, subsets of which are included in Figures 7-11, demonstrates non-uniformity below 5% of a pixel.

The spectral resolution of SWIS is established through the measurement of spectral response functions (SRF), with representative measurements shown in Fig. 7 covering the ranges of 400-520 nm, 950-720 nm and 1400-1470 nm. When compiled with other similar SRF measurements, they indicate that the full-width at half-maximum (FWHM) variation through field is < 2.5% of a pixel for all wavelengths. The monochrometer artifacts in Fig. 7 for the longer wavelengths will be fixed in future measurements. The curvature (smile) of a monochromatic slit image is shown in Fig. 6. A small tilt (4% of a pixel) has been subtracted to display the residual smile of ~5% of a pixel.

Spatial resolution is assessed through the measurement of the cross-track and along-track spatial response functions (CRF and ARF) through wavelength for various field positions. This is accomplished by orienting a sub-pixel slit placed at the focal plane of a collimator illuminating the instrument aperture either parallel or perpendicular to the spectrometer slit. Fig. 9 shows a representative CRF for adjacent spatial pixels with wavelengths spanning the spectral range. The FWHM values are around 0.9 to 1.1 pixel units, with better than 5% non-uniformity through wavelength for all fields. Fig. 10 shows the centroid location of each CRF plotted against spectral channel. A net tilt of 2% was subtracted, as it will be corrected in final alignment, leaving a total non-uniformity (keystone) below 5% of a pixel.

The along-track scan, measured through focus, provides a measure of the telescope-to-spectrometer alignment. A representative ARF measurement is shown in Fig. 11. The vertical axis is normalized to unity while the horizontal axis has been converted to pixel (slit) width units. In flight, this ARF measurement would be convolved with motion blur. The SWIS ARF FWHM resolution is on the order of 1.0 to 1.1 times the slit width with little variation through wavelength.

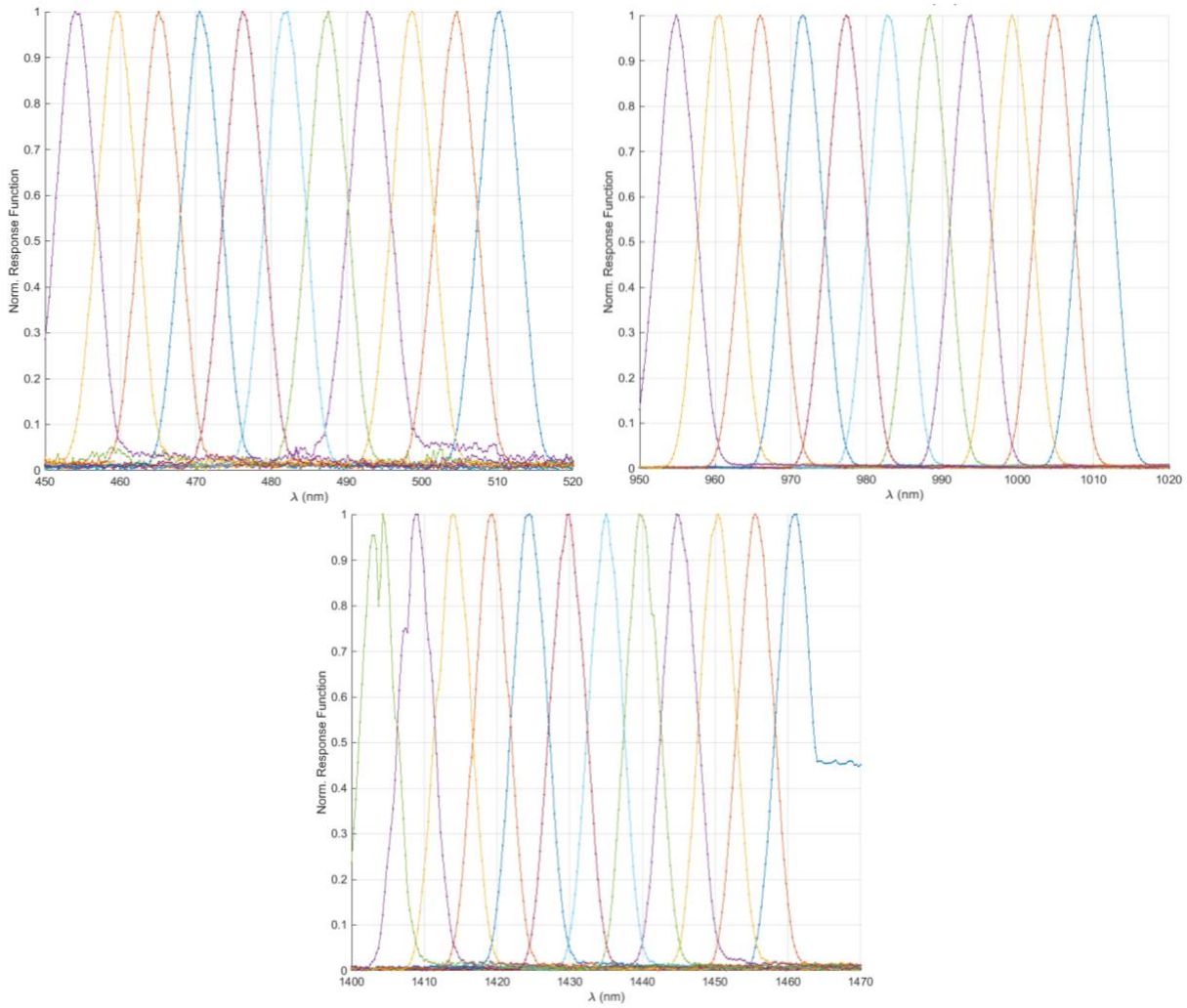

Fig. 7: Spectral response functions (SRFs) for the middle of the field of view spanning 70 nm at 485 nm (top left), 985 nm (top right) and 1435 nm (bottom). The SRF FWHM non-uniformity through field is <2.5% for all wavelengths.

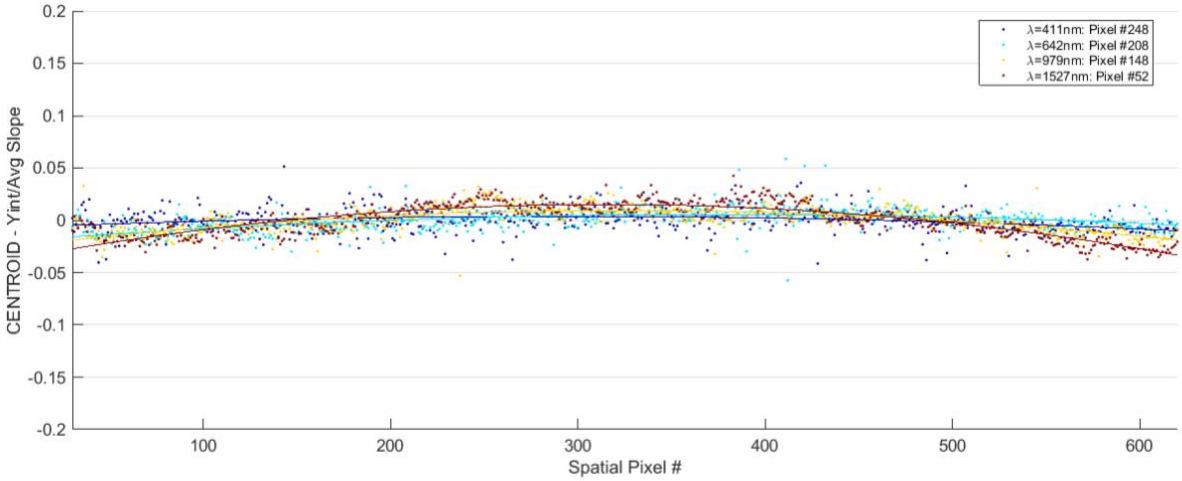

Fig. 8: Scatter plot of spectral channel centroids as a function of spatial location for several wavelengths. A small tilt (4% of a pixel) has been subtracted to display the residual smile of <5% of a pixel.

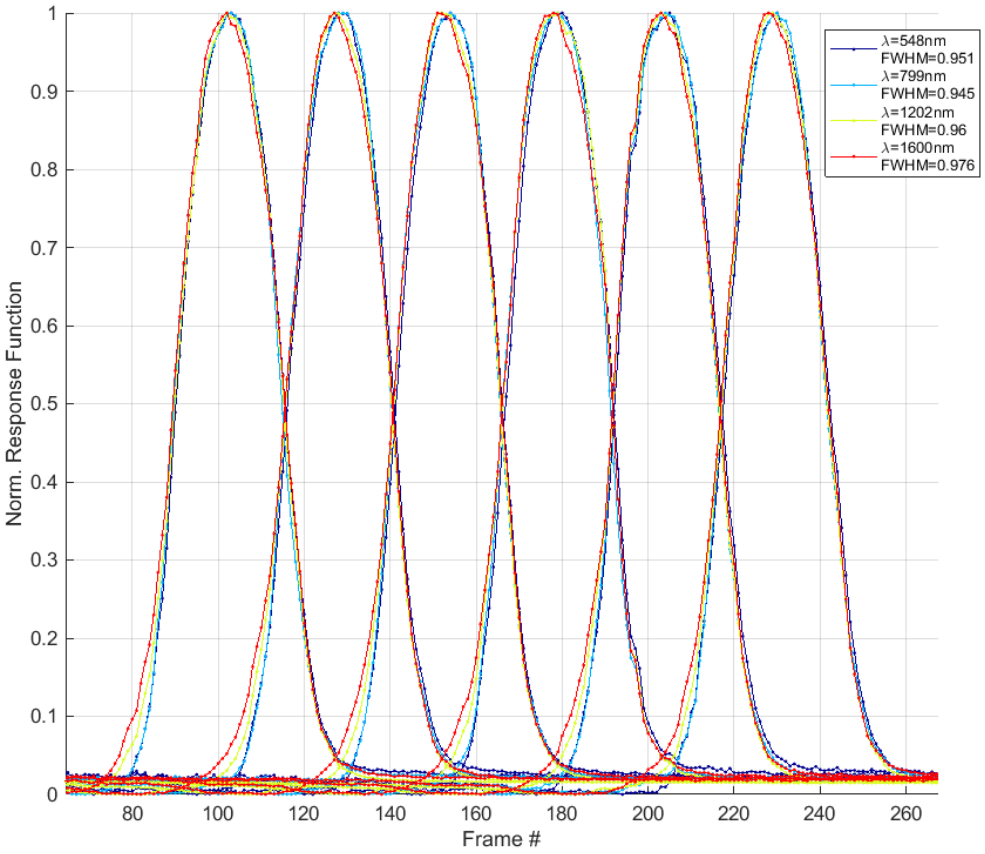

Fig. 9: Typical cross-track response functions (CRFs) for adjacent pixels and several wavelengths (0° Field). Here, the FWHM values are ~1.0 pixel units with good uniformity through wavelength.

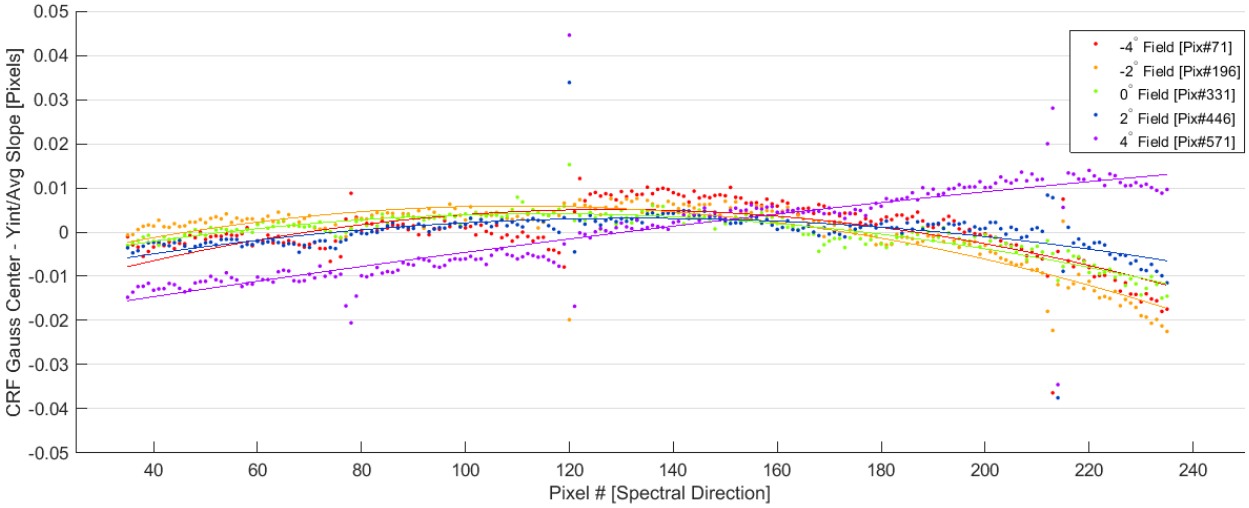

Fig. 10: Cross-track response function (CRF) centroids as a function of spectral channel for five field points spanning the instrument FOV. The CRF FWHM non-uniformity through wavelength is <5% of a pixel for all fields.

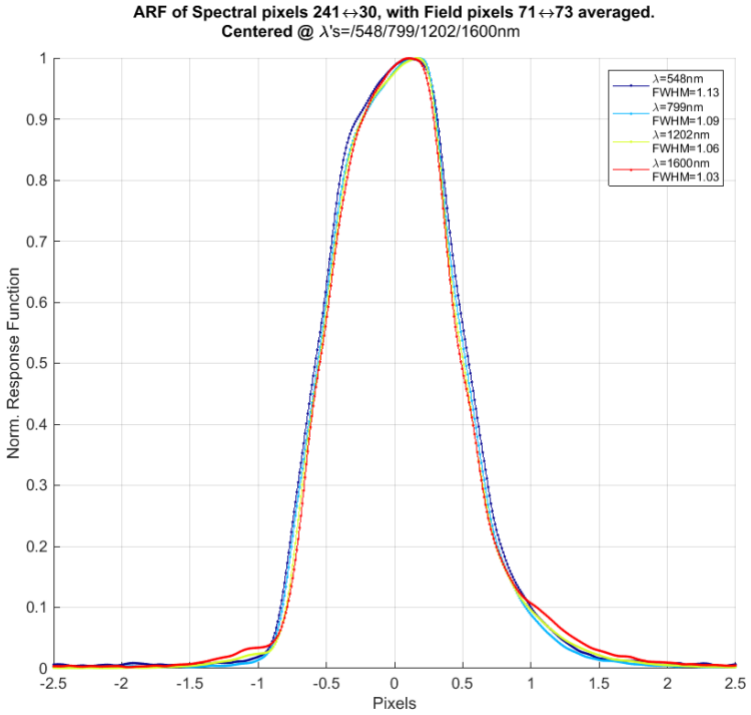

Fig. 11: Along-track Response Function at the edge of the field for several wavelengths (no motion smear).

4. CONCLUSIONS

We present a science-grade imaging spectrometer design suitable for CubeSat applications. The design advances the state of the art in compact sensors of this kind in terms of size and spectral coverage.

Key laboratory measurements have demonstrated that the SWIS optomechanical system meets its resolution and uniformity specifications. Further refinement of the measurements and final instrument-level calibration results will await the specially designed SWIS electronics that will provide lower noise levels.

The current spacecraft configuration conceptual model is favorable for accommodation of SWIS in a 6U CubeSat frame (REF). Future work will include development of a preliminary spacecraft bus and bus interface design and a refined thermal model.

ACKNOWLEDGMENTS

The research in this paper was performed at the Jet Propulsion Laboratory, California Institute of Technology under contract with the National Aeronautics and Space Administration. Reference herein to any specific commercial product, process, or service by trade name, trademark, manufacturer, or otherwise, does not constitute or imply its endorsement by the United States Government or the Jet Propulsion Laboratory, California Institute of Technology. Development of the CHROMA detector array and linear variable anti-reflection coating is in collaboration with Teledyne Scientific & Imaging under the leadership of Dr. Jianmei Pan. We are indebted to our science collaborators, Thomas Painter of JPL and Heidi Dierssen of the University of Connecticut, for framing the SWIS science investigation. We also thanks and acknowledge the SWIS team: Robert O. Green, Michael Eastwood, Johannes Gross, Peter Sullivan, Elliott Liggett, Christine Bradley, Zachary Small and Sander Zandbergen for their contributions.

REFERENCES

[1] Green, R. O., et al, "Imaging Spectroscopy and the Airborne Visible/Infrared Imaging Spectrometer (AVIRIS)," Remote Sensing of the Environment 65(3), 227-248 (1998).

[2] Simi, C., Reith, E., Olchowski, F., "The Mapping Reflected-energy Sensor - MaRS: A New Level of Hyperspectral Technology," Proc. SPIE 7457, 745703 (2009).

[3] Bender, H. A., Mouroulis, P., Green, R. O., Wilson, D. W., "Optical design, performance and tolerancing of next-generation airborne imaging spectrometers," Proc. SPIE, 7812, 78120P (2010).

[4] Mouroulis, P. et al, "Portable Remote Imaging Spectrometer coastal ocean sensor: design, characteristics, and first flight results," Appl. Opt. 53(7), 1363-1380 (2014).

[5] Green, R. O., et al., "The Moon Mineralogy Mapper (M3) imaging spectrometer for lunar science: Instrument description, calibration, on-orbit measurements, science data calibration and on-orbit validation," J. Geophys. Res. 116, E00G19 (2011).

[6] Mouroulis, P., Green, R. O., Wilson, D. W., "Optical design of a coastal ocean imaging spectrometer," Opt. Express 16, 9087-9095 (2008).

[7] Dierssen, H., et al, "Space station image captures a red tide ciliate bloom at high spectral and spatial resolution," Proc. Natl. Acad. Sci. 112, 14783-14787 (2015).

[8] Dozier, J., Green, R. O., Nolin, A. W., Painter, T. H., "Interpretation of snow properties from imaging spectrometry," Remote Sensing of Environment, 113, 525-537 (2009).

[9] Painter, T. H., et al, "Imaging spectroscopy of albedo and radiative forcing by light absorbing impurities in mountain snow," J. Geophys. Res., 118(17), 9511-9523 (2013).

[10] Bender, H. A., et al, "Snow and Water Imaging Spectrometer: development of a CubeSat-compatible instrument," Proc. SPIE 9881, 98810V (2016).

[11] Green, R. O., "Spectral calibration requirement for Earth-looking imaging spectrometers in the solar-reflected spectrum," Appl. Opt. 37, 683-690 (1998).

[12] Mouroulis, P., Van Gorp, B., Green, R. O., Wilson, D. W., "Optical design of a CubeSat-compatible imaging spectrometer," Proc. SPIE, 9222, 92220D (2014).

[13] Bender, H. A., et al, "Snow and Water Imaging Spectrometer (SWIS): Optomechanical and system design for a CubeSat-compatible instrument," Proc. SPIE 9611, 961103 (2015).

[14] http://www.syrlinks.com/en/products/cubesats/hdr-x-band-transmitter.html